Journal of Materials Chemistry B

ROYAL SOCIETY OF CHEMISTRY

PAPER

View Article Online
View Journal | View Issue

Cite this: J. Mater. Chem. B, 2023, 11, 2234

Mechanically robust and highly bactericidal macroporous polymeric gels based on quaternized *N*,*N*-(dimethylamino)ethyl methacrylate possessing varying alkyl chain lengths†

Amit Kumar,[a] Jyoti Sharma,[b] Preeti Srivastava[b] and Leena Nebhani *[a]

In this paper, macroporous antimicrobial polymeric gels (MAPGs) functionalized with active quaternary ammonium cations attached to varying hydrocarbon chain lengths have been fabricated. Apart from the change in the alkyl chain length attached to the quaternary ammonium cation, the amount of crosslinker was also varied during the fabrication of the macroporous gels. The prepared gels were characterized using Fourier transform infrared spectroscopy, X-ray photoelectron spectroscopy, field emission scanning electron microscopy (FE-SEM) and swelling studies. In addition, the mechanical properties of the fabricated macroporous gels were studied using compression and tensile testing. The antimicrobial activity of the gels has been determined for Gram-negative bacteria (*Escherichia coli*, *Pseudomonas aeruginosa*) as well as Gram-positive bacteria (*Bacillus subtilis*, *Staphylococcus aureus*). Antimicrobial activity, as well as the mechanical properties of the macroporous gels, was found to be influenced by the alkyl chain length attached to the quaternary ammonium cations as well as by the amount of crosslinker used for the fabrication of the gel. In addition, on increasing the alkyl chain length from C4 (butyl) to C8 (octyl), the effectiveness of the polymeric gels increased. It was observed that the gels derived using a tertiary amine (NMe_2) containing monomer showed relatively low antimicrobial activity as compared to the gels obtained using quaternized monomers (C4 (butyl), C6 (hexyl), and C8 (octyl)). The gels based on the quaternized C8 monomer displayed the highest antimicrobial activity and mechanical stability as compared to the gels based on the C4 and C6 monomers.

Received 12th October 2022,
Accepted 22nd January 2023

DOI: 10.1039/d2tb02178a

rsc.li/materials-b

1. Introduction

The development of multidrug resistance in microbes has become one of the severe threats to public health.[1,2] Recently, the World Health Organization has reported a list of pathogens that are the most threatening to human health.[3] The occurrence of antibiotic-resistant microbes which can be present in the environment (soil, water, and atmosphere)[4] is arguably a well-known concern. Thus, the presence of these antibiotic-resistant bacteria is the genesis of health problems worldwide.[5] Water-based systems are recognized to be one of the main domains for these types of microbes.[6] Numerous concerns and steps have been adopted for the purification of such types of water-based systems having pathogenic occurrences. Despite all efforts, many Gram-negative[7] and Gram-positive bacteria (for example, methicillin-resistance *Staphylococcus aureus*)[8] have acquired antibiotic resistance. To combat these threatening bacteria, the development of new antimicrobial systems based on polymers and nanoparticles is an essential requirement. There are several representative examples based on a polymeric system that can be utilized to overcome the problems related to antimicrobial resistance in bacteria, such as amphiphilic block copolymers,[9–12] polypeptide-based systems,[13–16] and nanoparticle-based systems.[17–20] Lam *et al.* designed structurally nanoengineered antimicrobial polymers based on peptides exhibiting excellent antimicrobial activity to Gram-negative bacteria including ESKAPE, colistin-resistance, and multidrug resistance (MDR) pathogens.[14] Similarly, Shirbin *et al.* have reported polypeptide-based macroporous cryogels with an in-built antimicrobial property for water purification applications. Other than peptide-based materials good structural

[a] Department of Materials Science and Engineering, Indian Institute of Technology Delhi, Hauz Khas, New Delhi-110016, India.
E-mail: Leena.Nebhani@mse.iitd.ac.in
[b] Department of Biochemical Engineering and Biotechnology, Indian Institute of Technology Delhi, Hauz Khas, New Delhi-110016, India.
E-mail: preeti@dbeb.iitd.ac.in

† Electronic supplementary information (ESI) available. See DOI: https://doi.org/10.1039/d2tb02178a

activities have also been reported using amphiphilic polymers.[21] Namivandi-Zangeneh *et al.* discussed the development of new antimicrobial polymers with amphiphilic ternary copolymers having potency against Gram-negative pathogens with low cytotoxicity.[9] Likewise, there have been other reports on using nanoparticles, for example, Li *et al.* demonstrated the use of functionalized gold nanoparticles as antimicrobial agent against multi-drug-resistance pathogenic bacteria with low toxicity to mammalian cells.[17] Out of all these, cationic amphiphilic polymer-based systems have emerged as promising antimicrobial agents for combating both Gram-negative and Gram-positive bacteria. These systems primarily consist of cationic and hydrophobic moieties which are important for providing interaction with the bacterial cell wall as well for the disruption of the bacteria cell wall.[22–28] It is worth mentioning that the length of the hydrophobic alkyl chain plays a crucial role in the bactericidal activity of the cationic polymer system.[17,29–32]

In this study, we have synthesized macroporous antimicrobial polymeric gels (MAPGs) bearing quaternary ammonium functionalities containing an alkyl group of varying chain length in a facile manner. In our previous work, we have studied in detail macroporous polymeric gels (MAPGs) containing the C6 alkyl chain and a comparison of its antimicrobial properties with respect to a similar conventional hydrogel. In the current study, the alkyl chain length has been varied from butyl, hexyl to the octyl group. In addition, MAPGs containing different alkyl chains attached to the quaternary ammonium cation were also varied in crosslinking density. All the macroporous gels were also studied for their mechanical properties and it has been clearly observed that Young's modulus increases as the alkyl chain length increases. All these macroporous gels containing different alkyl chain lengths as well as different crosslinker ratios were studied for antibacterial properties, and it was observed that the antimicrobial activity increases as the alkyl chain length increases from butyl to octyl due to increased hydrophobic interactions with the bacterial cell wall, which results in membrane disruption.

2. Experimental

2.1. Materials and methods

1-Bromooctane (TCI; >98%), 1-bromohexane (TCI; >98%), 1-bromobutane (TCI; >98%), *N*,*N*-(dimethylamino)ethyl methacrylate (DMAEMA) (TCI; >98.5%), oligo(ethylene glycol)dimethacrylate (OEG-DMA) M_n 550 g mol^{-1} (Aldrich; 98%), ammonium persulfate (APS) (TCI; >99%), *N*,*N*,*N*′,*N*″,*N*″-pentamethyldiethylenetriamine (PMDETA) (TCI; >99%), chloroform ($CHCl_3$) (Fisher Scientific), acetonitrile (ACN) (Fisher Scientific), LIVE/DEAD™ cell vitality assay kit (Thermo Fisher Scientific) and diethyl ether (DEE) (Merck) were used as received. Milli-Q water with a resistivity of >18 MΩ cm was used in all the experiments.

2.2. Characterization methods

Nuclear magnetic resonance (NMR). A Bruker AC 400 MHz Fourier transform nuclear magnetic resonance (FT-NMR) spectrometer has been utilized to obtain the ^{1}H and ^{13}C NMR spectra of the monomer samples. A deuterated solvent D_2O (Sigma-Aldrich, 99.9 atom % D) was used as a reference solvent, and the sample concentration was 10–20 mg mL^{-1}.

Fourier transform infrared (FTIR) spectroscopy. A Thermo Fisher Scientific FTIR instrument (NICOLET, iS50 FT-IR) was used to record the attenuated total reflection (ATR) infrared spectra. A film of dried gel samples was used for the ATR analysis. All spectra were collected in the 4000–400 cm^{-1} wavenumber region with a resolution of 4 cm^{-1}.

X-ray photoelectron spectroscopy. X-ray photoelectron spectroscopy (XPS) was performed on a PHI 5000 Versa Probe III X-ray photoelectron spectrophotometer (Physical Electronics) using an Al Kα X-ray source and an argon ion gun.

Flow cytometer. A Becton Dickinson (BD) FACS Calibur flow cytometer has been used for identifying dead cell populations. Propidium iodide (Sigma), a membrane-impermeant dye was used to exclude dead cells from the viable cell population. Propidium iodide (PI) has a 488/615 nm maxima of excitation/emission and 488 nm (blue laser) is optimal for PI excitation. The flow cytometer instrument was adjusted to read the PI fluorescence, the FL-2 channel was used and the flow rate of 500 events per s was adjusted.

Confocal microscope. A Leica TCS SP8 (Germany) inverted fluorescent confocal microscope was used to image the cells stained with dye. The images were captured using a CCD camera through a 40× oil objective. The images were recorded as tiff files and were analyzed using Leica Las X software.

Field emission scanning electron microscopy (FESEM). The surface morphology of the dried gels was investigated using a JSM-7800F prime instrument at an accelerating voltage of 10 keV. Samples were directly mounted on carbon tape and were coated with a thin layer of gold. The FESEM of the gel samples was taken after freeze-drying the swollen gels.

Mechanical testing. The mechanical strength of the swollen gel samples was assessed by compression and tensile testing using a universal testing machine (Zwick Roell) with a load cell of 1 kN. All the compression tests were performed at room temperature at a strain rate of 2 mm min^{-1}, and the gel dimensions were measured with vernier callipers. The compressive Young's modulus of the scaffolds was determined using the slope of the initial elastic region of stress *vs.* strain plots. For tensile testing, the sample was dumbbell-shaped and was gripped between moving upper grips and fixed lower grips. The experiments were conducted in triplicate, and the average values are reported.

2.3. Synthesis of quaternary ammonium (QA) monomers

1-Bromooctane (0.153 mol), 1-bromohexane (0.153 mol) or 1-bromobutane (0.153 mol) were added to a solution of DMAEMA (0.127 mol) in 150 mL of ACN:$CHCl_3$ (2 : 1 volume ratio) solvent mixture. The reaction mixture was stirred at 40 °C for 16 h. The contents were poured slowly into a beaker of cold diethyl ether (2 L) to precipitate the product. The filtrate was collected, washed with diethyl ether (*ca.*1 L), and was dried under vacuum for 24 h to yield the pure QA monomers as a white solid, which were analyzed. The quaternary monomers

based on 1-bromooctane, 1-bromohexane and 1-bromobutane are designated as C8, C6, and C4 respectively. The yield of the different monomers obtained is as follows: C8 yield 34.3 g (0.097 mol), C6 yield 35.3 g (0.109 mol), C4 yield 32.5 g (0.110 mol). The purity of the monomers was confirmed by ^{1}H and ^{13}C NMR spectroscopy. The ^{1}H and ^{13}C NMR spectra of all three monomers are shown in Fig. S1–S3 (ESI†).

C4: ^{1}H NMR (400 MHz, D_2O) δ 6.18 (d, 1H), 5.80 (d, 1H), 4.65 (t, 2H), 3.79 (t, 2H), 3.42 (t, 2H), 3.18 (s, 6H), 1.96 (s, 3H), 1.80 (m, 2H), 1.40 (m, 2H), 0.97 (t, 3H); ^{13}C NMR (100 MHz, D_2O) δ 168.5, 135.2, 127.6, 65.2, 62.1, 58.4, 51.2, 23.9, 19.0, 17.2, 12.7.

C6: ^{1}H NMR (400 MHz, D_2O) δ 6.19 (d, 1H), 5.81 (d, 1H), 4.65 (t, 2H), 3.80 (t, 2H), 3.42 (t, 2H), 3.19 (s, 6H), 1.97 (s, 3H), 1.81 (m, 2H), 1.36 (m, 6H), 0.90 (t, 3H); ^{13}C NMR (100MHz, D_2O) δ 168.5, 135.2, 127.7, 65.4, 62.1, 58.4, 51.3, 30.4, 25.1, 21.9, 21.7, 17.3, 13.2.

C8: ^{1}H NMR (400 MHz, D_2O) δ 6.18 (d, 1H), 5.80 (d, 1H), 4.64 (t, 2H), 3.78 (t, 2H), 3.41 (t, 2H), 3.18 (s, 6H), 1.96 (s, 3H), 1.80 (m, 2H), 1.33 (m, 10H), 0.88 (t, 3H); ^{13}C NMR (100 MHz, D_2O) δ 168.4, 135.1, 127.8, 65.3, 62.1, 58.4, 51.4, 31.0, 28.2, 25.5, 22.02, 22.00, 17.3, 14.1, 13.4.

2.4. Fabrication of macroporous antimicrobial polymeric gel

The C8, C6, and C4 monomers were mixed with crosslinker OEG-DMA in a glass vial followed by the addition of Milli-Q water (1.5 g) for the dissolution of the contents. Then, PMDETA was added to the solution. The redox initiator APS was added last, and the solution was mixed thoroughly. All the contents were transferred to a polypropylene syringe (3 mL and 9 mm diameter). The polymerizable media was immediately frozen in liquid N_2 and was kept in a freezer at -20 °C for 3 days to obtain the MAPGs. The gels were purified by immersing in Milli-Q water (100 mL) for 10 h which included periodic changing of the solvent every 2 h. The sample designation for the MAPGs prepared using different crosslinker ratios are C4-5 for the MAPGs containing the QA monomer possessing a butane chain and having 5 equivalents of crosslinker with respect to initiator. All other MAPGs are also designated in a similar way. Table S1 (ESI†) summarizes the various QA monomers as well as the quantity of crosslinker, initiator and PMDETA used for the preparation of the MAPGs.

2.5. Swelling studies on MAPG

A gravimetric method was utilized to estimate the swelling kinetics of the MAPGs. Briefly, the lyophilized gel was weighed (M_0). After being immersed in DI water at ambient temperature for predetermined time intervals, the sample was blotted with filter paper to remove the excess water on the surface and weighed (M_t). The sample was measured in triplicate and the swelling degree was calculated according to the following equation:

$$\text{Swelling degree} = M_t/M_0 \quad (1)$$

2.6. Antimicrobial assay

The Gram-negative *Escherichia coli* and *Pseudomonas aeruginosa* and the Gram-positive *Bacillus subtilis* and *Staphylococcus aureus* were used in the present study to test the antimicrobial activity of the gels. A single colony was inoculated in 5 mL of LB medium at 30 °C with shaking at 180 rpm overnight. About 100 μL of the overnight culture was mixed with 5 mL of fresh LB medium and was allowed to grow until $OD_{600} \approx 1$, which corresponds to 1×10^8 CFU mL^{-1}. About 1 mL of the culture was centrifuged at 8000 rpm. The pellet was washed twice and was resuspended in PBS solution, then serially diluted to 1 : 100 000. The bacterial concentration in the last dilution tube was maintained at 10^4 cells per mL. All 16 fully swollen gels (NMe_2-2.5, NMe_2-5, NMe_2-10, NMe_2-15, C4-2.5, C4-5, C4-10, C4-15, C6-2.5, C6-5, C6-10, C6-15, C8-2.5, C8-5, C8-10, C8-15) were cut into thin slices with the help of a sterile blade and each gel was added into the tubes containing bacterial cells prepared above. The tubes were incubated at 30 °C for 60 minutes with shaking at 180 rpm. After treatment, 100 μL of sample was collected from each gel tube and plated onto LA plates. The plates were incubated for 24 h at 30 °C. The colonies obtained were counted for each gel sample. The final number of colonies obtained for the 10^8 CFU mL^{-1} sample was calculated by multiplying the dilution factor by the number of colonies obtained in the LA plate. The bacterial preparation without gel was used as a positive control and only PBS solution was used as a negative control. All the experiments were performed in triplicate and were repeated three times.

For calculating the % reduction, the CFU/100 μL values were multiplied by the unit conversion factor to obtain the CFU mL^{-1} value. Then, the CFU mL^{-1} values were multiplied by the dilution factor to obtain the final values. The final values of the triplicates were used to obtain the average value and the standard deviation.

% Reduction values were calculated by the following formula:

$$\%\,\text{Reduction} = \left(\frac{\text{Initial CFU} - \text{final CFU}}{\text{initital CFU}}\right) \times 100 \quad (2)$$

2.7. Flow cytometry experiment

For the flow cytometry analysis, bacterial cells were grown up to $OD_{600} \sim 1$. The cells were centrifuged at 8000 rpm for 10 minutes and the cell pellet was washed twice with PBS. The cells were diluted to obtain a concentration of 10^6 cells per mL. The cells were incubated with the polymeric gels for 60 minutes. About 500 μL of the sample was taken from each tube with or without vortexing. In each treated sample, propidium iodide (PI) was added. PI can penetrate dead cells due to their compromised membranes. It intercalates between double-stranded DNA and produces red fluorescence. About 20 μL of PI dye (from 5 μg mL^{-1} stock solution) was added to each tube and incubated in the dark for 10 minutes. The antimicrobial activity of the gels was validated by the percentage of dead cells present in the samples and was evaluated using a flow cytometer.

2.8. Confocal microscopy

For visualizing the bacterial cells on the gel, confocal microscopy was performed. 100 μL sample tubes containing the gels were incubated for 60 minutes. From each tube, 100 μL of the sample supernatant was collected before vortexing and after

vortexing, 2 μL of PI dye from the 10 μg mL^{-1} stock solution (Sigma, USA) for visualization of dead cells and 2 μL resazurin dye from the 0.02% stock solution (Sigma, USA) for visualization of live cells was added in each collected sample separately followed by incubation in a dark place for 10 minutes. For the slide preparation, a drop (10 μL) from each sample tube was placed at the centre of the microscope slide and the coverslip was placed over it carefully to avoid air bubbles. The excess sample was removed with a paper wipe. Then, transparent nail polish was carefully applied on the edges for sealing. Once the nail polish was dried, the slides were visualized under a confocal microscope.

2.9. Statistical analysis

One-way ANOVA and student's *t*-test (two-tailed) were performed where differences between data were regarded as statistically significant with *p*-values < 0.05.

3. Results and discussion

3.1. Macroporous antimicrobial polymeric gel (MAPG)

Previously, our research group has reported the fabrication of a MAPG by free radical polymerization of a quaternary ammonium (**QA**) monomer bearing a hexyl group, an oligoethylene glycol-dimethacrylate (**OEG-DMA**) crosslinker, and ammonium peroxydisulfate (**APS**)/*N*′,*N*′,*N*′,*N*″,*N*″-pentamethyldiethylenetriamine (**PMDETA**) as a redox initiator, under cryogenic conditions.[32] The monomer bearing the hexyl group was selected, as a judicious combination of cationic and hydrophobic groups to display good antimicrobial activity. It has been mentioned that sufficient hydrophobicity is a requisite to result in membrane disruption, while the cationic nature of the ammonium moiety enables interaction with the anionic bacterial cell wall.[32] In view of the same, a variety of **MAPGs** have been fabricated in the present study, which differ in crosslinker ratio, as well as in chain length of the alkyl substituent in the **QA** monomer. The **QA** monomers bearing hydrophobic tails of butyl (designated as **C4**), hexyl (designated as **C6**), and octyl (designated as **C8**) groups were first synthesized *via* a quaternization reaction between 2-(dimethylamino)ethyl methacrylate and 1-bromobutane, 1-bromohexane, and 1-bromooctane respectively (Fig. 1). It is to be noted that the preparation and purification of the monomers was facile. The successful preparation of the **QA** monomers was confirmed by ^{1}H and ^{13}C NMR spectroscopy and the labelled spectra with the integration values are presented as Fig. S1, S2, and S3 in ESI.†

The synthesized **QA** monomers were utilized to fabricate **MAPGs** by subjecting them to free radical polymerization with **OEG-DMA** as a crosslinker (Fig. 2) and the compositions adopted for the reactants are presented in Table S1 (ESI†). The macroporous morphology of the gels is the result of ice crystal formation at sub-zero temperatures, which acts as porogen within the aqueous polymerizable media and this method of preparing macroporous gel is called cryogelation.[18,33–36]

The MAPGs prepared in the present work are white in color as shown in Fig. S6–S9 (ESI†) and display buoyancy in water.

It is worth mentioning that the fabrication of gels requires simple mixing of the starting materials, which is an important feature for developing a prototype filter or cartridge based on MAPGs.

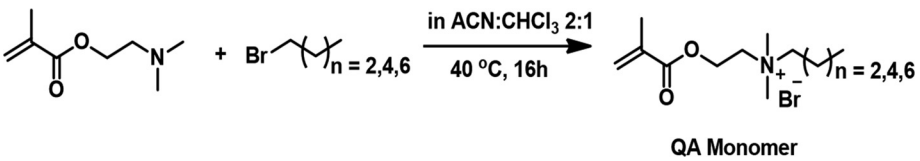

Fig. 1 Reaction scheme representing the synthesis of the quaternary ammonium monomers differing in chain length of the alkyl substituents.

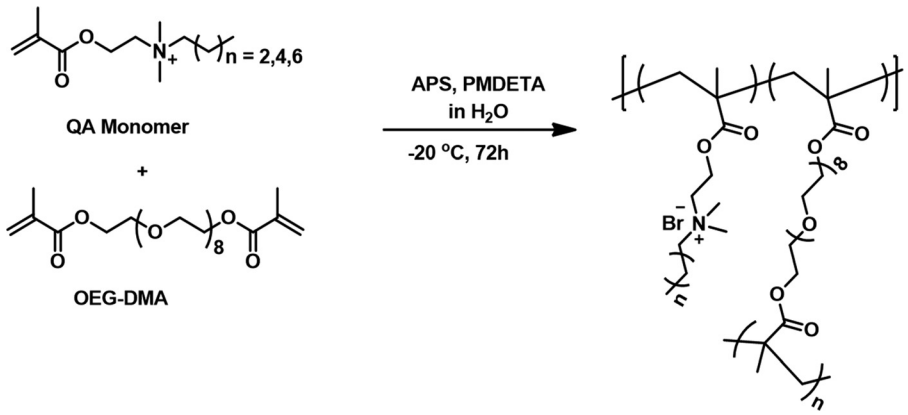

Fig. 2 Reaction scheme representing the fabrication of the macroporous antimicrobial polymeric gel (MAPG) bearing alkyl groups of different chain lengths *via* free radical polymerization at sub-zero temperatures.

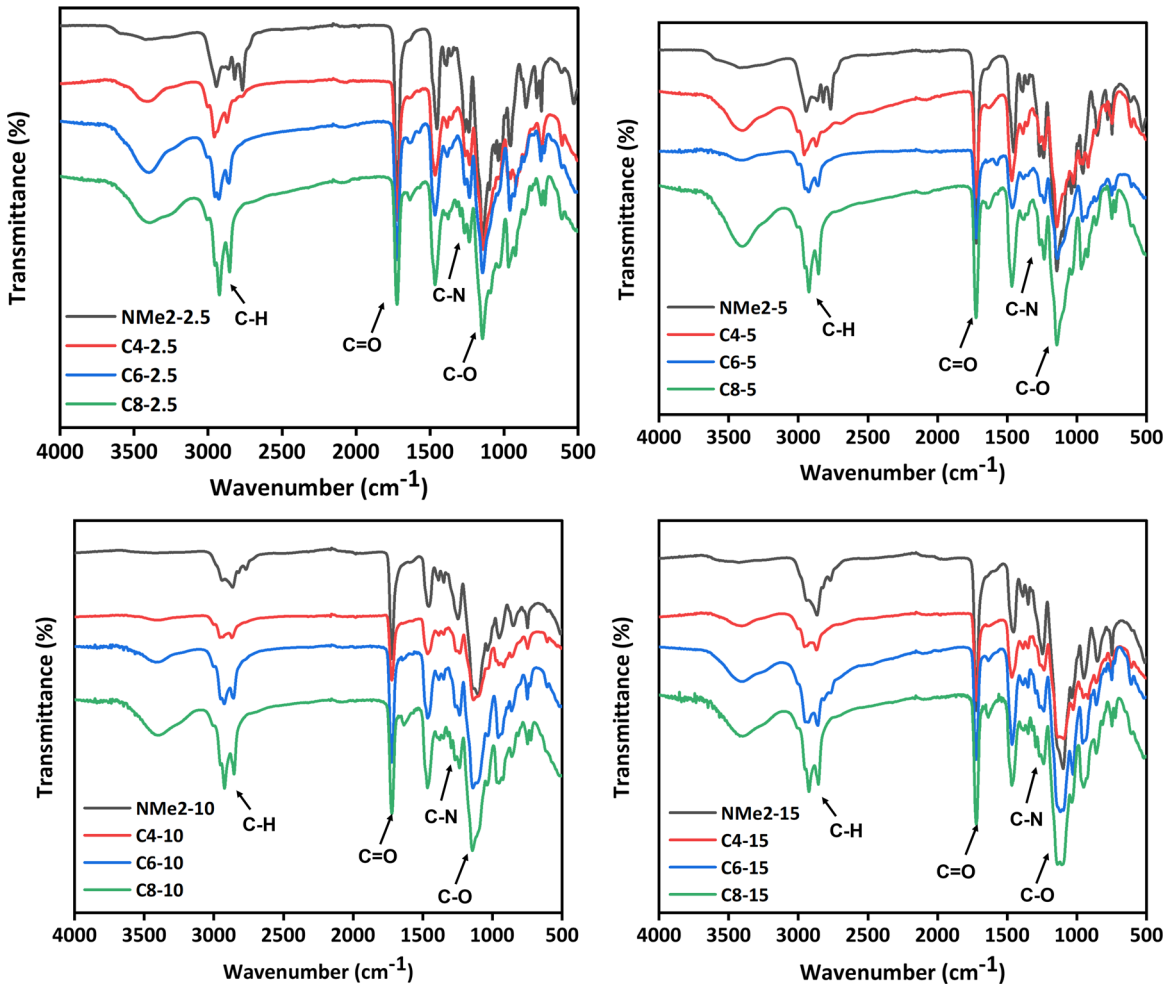

Fig. 3 FTIR spectra of the MAPGs (a) NMe2-2.5, C4-2.5, C6-2.5, C8-2.5 (b) NMe2-5, C4-5, C6-5, C8-5 (c) NMe2-10, C4-10, C6-10, C8-10 (d) NMe2-15, C4-15, C6-15, C8-15.

The synthesized gels were characterized using FTIR spectroscopy and the spectra has been presented in Fig. 3. The FTIR spectra recorded for all gel samples show band in the range 2850–2950 cm^{-1} for all gels which is attributed to a C–H stretching vibration. Further, intense absorption band at 1720–1730 cm^{-1} attributed to the stretching vibration of the

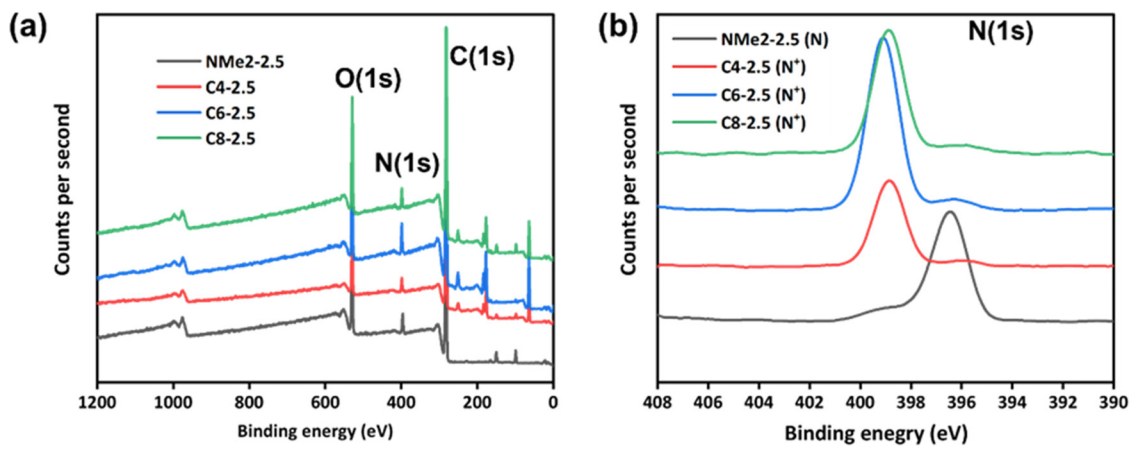

Fig. 4 (a) X-ray photoelectron spectra of the NMe2-2.5, C4-2.5, C6-2.5, and C8-2.5 gel samples; high resolution XPS of the NMe2-2.5, C4-2.5, C6-2.5, and C8-2.5 gel samples (b) N(1s).

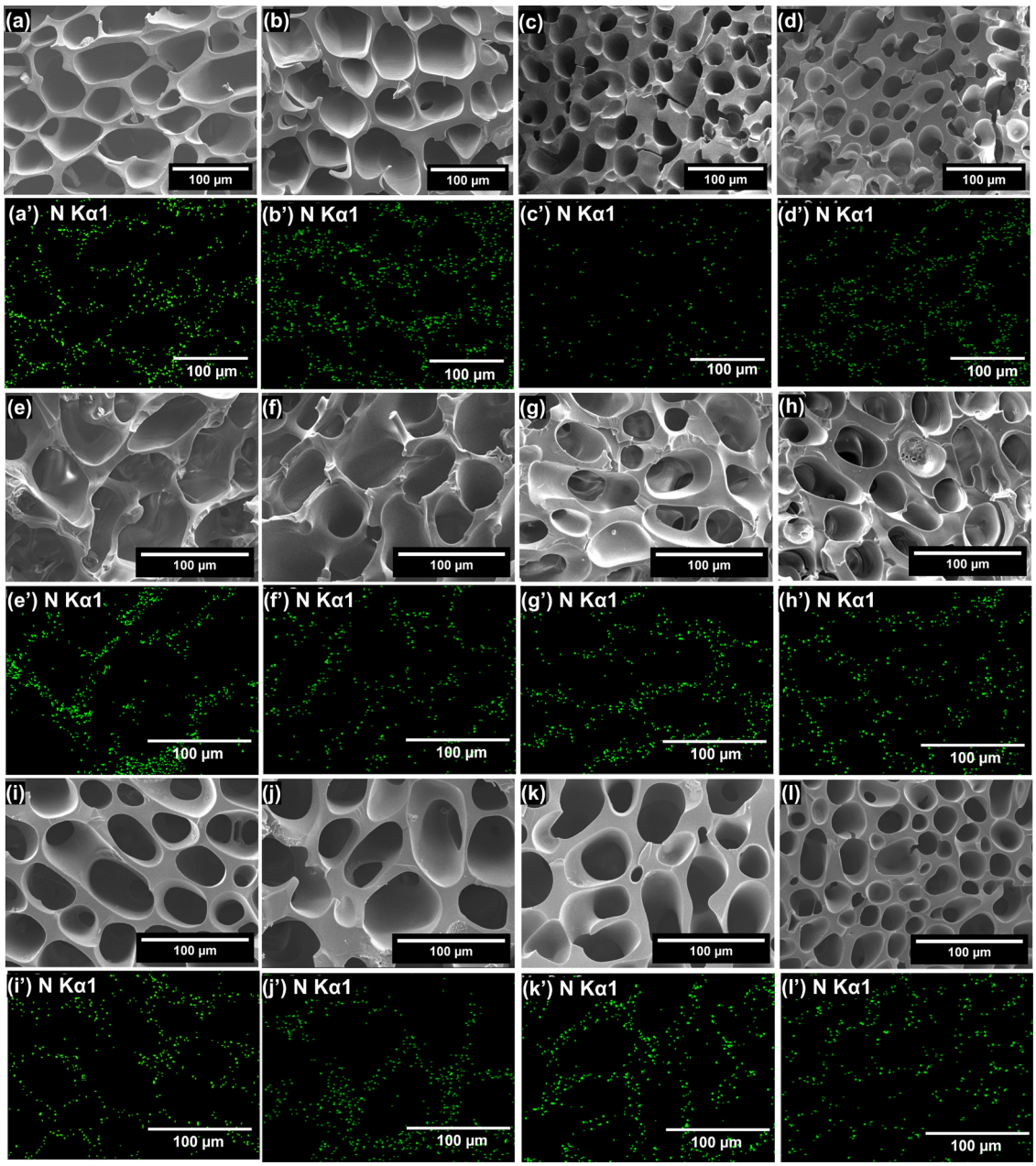

Fig. 5 SEM micrographs and nitrogen mapping from the EDX spectra of MAPG (a, a′) C4 having 2.5 eq. crosslinker (b, b′) C4 having 5 eq. crosslinker (c, c′) C4 having 10 eq. crosslinker (d, d′) C4 having 15 eq. crosslinker (e, e′) C6 having 2.5 eq. crosslinker (f, f′) C6 having 5 eq. crosslinker (g, g′) C6 having 10 eq. crosslinker (h, h′) C6 having 15 eq. crosslinker (i, i′) C8 having 2.5 eq. crosslinker (j, j′) C8 having 5 eq. crosslinker (k, k′) C8 having 10 eq. crosslinker (l, l′) C8 having 15 eq. crosslinker.

carbonyl bond were observed. All NMe2, C4, C6, and C8 gels show strong absorption band at 1140 cm^{-1} attributed to the stretching vibration of the C–O bond. Further, the absorption band associated with C–H bending was observed at 1450 cm^{-1} for all gels. Furthermore, two weak bands at 1240 cm^{-1} and 1278 cm^{-1} were observed for the NMe2 gels which are attributed to the C–N stretching vibration. However, the C4, C6, and C8 gels show two weak bands at 1260–1270 cm^{-1} and 1230–1238 cm^{-1}, which corresponds to the C–N stretching vibration for the quaternized samples.

Further, gel samples designated as NMe2-2.5, C4-2.5, C6-2.5, and C8-2.5 were characterized by XPS analysis. Fig. 4(a) shows the overall XPS spectrum of the NMe2-2.5, C4-2.5, C6-2.5, and C8-2.5 gel samples. The high-resolution N(1s) spectra for the NMe2-2.5, C4-2.5, C6-2.5, and C8-2.5 gel samples are presented in Fig. 4(b). Peaks at binding energies N(1s) of 398.8 eV, 399 eV, and 399.1 eV were observed for the quaternized gels designated as C4-2.5, C6-2.5, and C8-2.5 respectively, which decreased to 396.4 eV for the unquaternized NMe2-2.5 gel sample. Fig. S4(c) (ESI†) displays the high-resolution C(1s) XPS spectra. Three

peaks, at ~281.2, 282.5, and 285.8 eV can be assigned to the C–C, C–N^+/C–N, and C=O bonds of the gel samples, respectively. From the high-resolution O(1s) spectra (Fig. S4d, ESI†), the two peaks at ~529.1 and 530.7 eV correspond to C–O and C=O respectively.

3.2. Morphological characterization of MAPGs

SEM analysis of the lyophilized MAPGs was performed, which confirmed the macroporous structure of the gels. The pore size distribution of the MAPGs was determined by using ImageJ software, and the micrographs of the MAPGs prepared using a variety of starting materials with varying compositions are presented in Fig. 5 and Fig. S5 (ESI†). The morphology and pore size distribution of the gels fabricated using *N*,*N*-(dimethylamino)ethyl methacrylate, the quaternized monomer with C4, C6, and C8 alkyl chain lengths and 2.5 eq. of the crosslinker is presented in Fig. 5(a, e and i) and Fig. S5(a) (ESI†). At 2.5 eq. of crosslinker, average pore sizes of 15 μm, and 53 μm have been obtained for the NMe_2, and C4 gels respectively, which further increases to 66 μm for the C6 gel. It is to be noted that the average pore size of the gels fabricated using monomers quaternized with the C4, and C6 alkyl chain lengths is higher as compared to gels derived from unquaternized monomers, which is attributed to the relatively higher interaction of the charged moiety with water, thereby increasing the size of the ice crystal template around the reactive solution resulting in higher porosity. Fig. 5(b, f and j) and Fig. S5(b) (ESI†) presents the morphology and pore size distribution of the gels fabricated using *N*,*N*-(dimethylamino)ethyl methacrylate, the quaternized monomer with C4, C6, and C8 alkyl chains and 5 eq. of the crosslinker. At 5 eq. of the crosslinker, average pore sizes of 8 μm, and 40 μm have been obtained for the NMe_2, and C4 gels respectively, which further increases to 42 μm for the C6 gel. Fig. 5(c, g and k) and Fig. S5(c) (ESI†) show the morphology and pore size distribution of the gel fabricated using *N*,*N*-(dimethylamino)ethyl methacrylate, the quaternized monomer with C4, C6, C8 alkyl chains with 10 eq. of the crosslinker. The results reveal that at 10 eq. of the crosslinker, the average pore sizes of 7.8 μm, and 30 μm have been obtained for the NMe2, and C4 gels, which further increases to 34 μm for the C6 gel. The morphology and pore size distribution of the gel fabricated using *N*,*N*-(dimethylamino)ethyl methacrylate, the quaternized monomer with C4, C6, and C8 alkyl chains with 15 eq. of the crosslinker is presented as Fig. 5(d, h and l) and Fig. S5(d) (ESI†). It can be observed that at 15 eq. of the crosslinker, an average pore size of 3 μm, and 25 μm have been obtained for the NMe_2, and C4 gels, which further increases to 31 μm for the C6 gel. For the C8 gel, at 2.5 eq. of the crosslinker, an average pore size of 52 μm has been obtained, which further reduces to 21 μm on increasing the amount of crosslinker to 15 eq. It is to be noted that the pore size of the gel is also influenced by the amount of crosslinker, and a reduction in porosity, thickening of the pore walls, as well as a reduced level of pore interconnectivity is observed on increasing the amount of crosslinker. This can be attributed to the decrease in network flexibility as well as pore size.

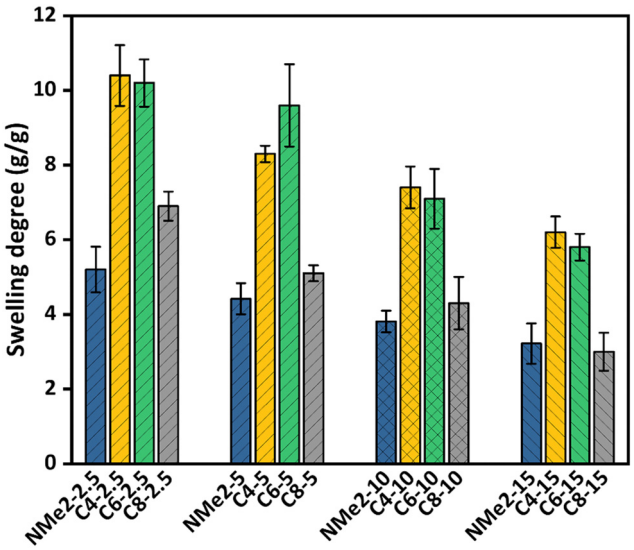

Fig. 6 Swelling degree for the MAPG bearing alkyl groups of different chain lengths and at varying crosslinking ratios.

A comparison of the results reveals that variation in the alkyl chain length influences the pore morphology of the MAPGs. On increasing the alkyl chain length from C4 to C6, an increase in the pore size with more pore interconnectivity has been observed which has been attributed to the reduction in the polymerization rate due to stearic hindrance, thereby leading to slow gelation and consequently to larger ice crystal formation which acts as a template. Further, as the length of the alkyl chain was extended to C8, a reduction in pore size with increasing wall thickness has been observed. This is a result of hydrophobicity associated with the C8 monomer, which repels water molecules, and leads to the formation of smaller ice crystal templates, as well as an increased rate of polymerization due to an increase in concentration (aggregation) in the monomer functionalized with the C8 alkyl chain length, which results in faster gelation, resulting in the formation of small pores with a thicker pore wall.[37,38]

Further, elemental analysis of the gel samples was performed using energy dispersive X-ray analysis (EDX) and the nitrogen mapping of the respective gels is shown in Fig. 5.

3.3. Swelling behavior of MAPGs

Swelling studies were performed on the MAPGs to further investigate the influence of the crosslinker ratio and alkyl chain length on the swelling behavior of the gels. It is expected that the gel network having a higher pore volume with interconnected pores will show higher swelling in water which can be due to a greater amount of free water in the larger pores. In addition, the network flexibility is expected to affect the swelling behavior of the MAPGs. It is believed that a lower crosslink density assists in the network expansion because of the flexible polymer chain, thereby leading to an increase in swelling degree on decreasing the amount of crosslinker. Further, hydrophobicity in the network additionally plays an important role in the swelling behaviour of the MAPGs, where it is expected that the hydrophobic gels will display relatively less swelling in water.

Table 1 Physical properties and antimicrobial activity of polymer gels against *E. coli*, *P. aeruginosa*, *S. aureus*, and *B. subtilis*

Samples	*E* (kPa)	Swelling degree (θ)	% Bacteria reduction			
			E. coli	*P. aeruginosa*	*S. aureus*	*B. subtilis*
NMe2-2.5	19.6 ± 11	5.2	91.6411	73.6567	52.6886	94.9181
NMe2-5	99.1 ± 42	4.4	88.3792	73.2835	52.4284	95.6320
NMe2-10	388 ± 40	3.8	85.0152	78.8806	59.6704	95.8420
NMe2-15	736 ± 84	3.2	94.2915	93.8806	54.6400	97.0180
C4-2.5	118 ± 24	10.4	89.2966	93.5820	100	99.1180
C4-5	401 ± 44	8.3	91.0805	94.9253	99.8699	99.2440
C4-10	563 ± 74	7.4	91.5392	93.3333	99.8799	99.6220
C4-15	1016 ± 68	6.2	95.4638	94.3283	99.0893	99.6640
C6-2.5	131 ± 19	10.2	99.7961	79.2720	99.6964	99.4960
C6-5	434 ± 38	9.6	99.4393	84.9253	99.6097	99.4960
C6-10	795 ± 22	7.1	99.6941	95.7213	99.9132	99.4960
C6-15	1225 ± 81	5.8	99.5922	95.7711	99.7398	99.8110
C8-2.5	142 ± 14	6.9	100	99.1791	100	99.5590
C8-5	404 ± 58	5.1	99.8470	99.5522	99.9566	99.8740
C8-10	832 ± 67	4.3	100	99.4029	99.9132	99.1600
C8-15	1446 ± 38	3.0	99.4393	99.6517	99.7831	99.4960

The results obtained from the swelling studies on the MAPGs are plotted in Fig. 6 and Fig. S6 (ESI†) and are tabulated in Table 1. Accordingly, it can be observed that the gels derived using the NMe2 monomer show relatively less swelling as compared to the swelling of the gels prepared using the quaternized monomers (C4, C6, and C8), which has been ascribed to the hydrophobic nature of the NMe2-based gels. In addition, the swelling degree of the NMe2-based gels further reduces from 5.2 to 3.2 on increasing the crosslinker ratio from 2.5 eq. to 15 eq.

The gel prepared using the quaternized monomer labelled as C4-2.5 shows a swelling degree of 10.4 like the swelling degree of 10.2 of the gel labelled as C6-2.5, which reduces to 6.9 for the C8-2.5 gels. Furthermore, the swelling degree of the C4-5 gel is 8.3, which increases to 9.6 for the C6-5 gels and reduces to 5.1 for the C8-5 gel. It is to be noted that, instead of having a long alkyl chain, the C6 gel has almost similar swelling to the C4 gel prepared using 2.5 eq. of the crosslinker and a higher swelling with a 5 eq. crosslinker amount. This is due to the larger as well as more interconnected pores found in the C6-2.5 and C6-5 gels, which dominate the overall hydrophobicity. However, the C4-10 and C4-15 gels have higher swelling as compared to the C6-10 and C6-15 gels, respectively. In this case, the overall hydrophobicity contributes more to the swelling than the pore size, resulting in the lower swelling of the C6-10 and C6-15 gels. In addition, it is to be noted that the C8 gels with all crosslinker ratios have lower swelling in water as compared to the C4 and C6 gels, which can be due to the lower pore size as well as the higher overall hydrophobicity of the octyl chain.

Furthermore, it is worth mentioning that for all the NMe2, C4, C6, and C8 gels, the swelling degree decreases with increasing the crosslinker amount from 2.5 to 15 eq., as shown in Fig. S7–S10 (ESI†), where it can be clearly seen that the gels with a higher crosslinker ratio show less swelling, which can be attributed to a reduction in the average pore size as well as the pore connectivity.

3.4. Mechanical properties of MAPGs

The mechanical properties of swollen MAPGs were determined under the uniaxial compression mode as well as using tensile testing. Previously it was found that porosity is an important factor that can affect the toughness of porous materials such as MAPGs. Furthermore, the crosslinker ratio can also affect the toughness of these porous materials. It is expected that the gels with a higher crosslink density will be mechanically tougher than the gels with a lower crosslink density. The Young's modulus (*E*) values of all the MAPGs are presented in Fig. 7(a) and the same are tabulated in Table 1, which were determined from the strain–stress graph shown in Fig. 7(b) and Fig. S11–S14 (ESI†). In the case of the gel fabricated using the *N*,*N*-(dimethylamino)ethyl methacrylate monomer at 2.5 eq. of the crosslinker, Young's modulus (*E*) of 19.6 ± 11 kPa was observed, which further increased to 736 ± 84 kPa on increasing the amount of the crosslinker to 15 eq. For the gels fabricated using the quaternized monomer with the C4 alkyl chain length at 2.5 eq. of the crosslinker, Young's modulus of 118 ± 24 kPa was observed, which further increases to 1016 ± 68 kPa on increasing the amount of crosslinker to 15 eq. Similar trends were observed in the case of the gels fabricated from the C6, and C8 monomers and the Young's modulus values are presented in Table 1. It is to be noted that the gels with a higher crosslink density are mechanically tougher. In addition, the hydrophobic alkyl chain in the network additionally plays an important role in deciding the mechanical behavior of the MAPGs, where it is expected that the gels with hydrophobic alkyl groups will be mechanically tougher than the gels without any alkyl chains. It can be observed that the gels derived using the NMe2 monomer are relatively less mechanically tough than the gels obtained using the quaternized monomers (C4, C6, and C8). Further, the strain–stress graph (Fig. 7b), Fig. S11–S14 (ESI†), and Table S2 (ESI†) from compression testing show that C8-2.5 gel does not break at all, while the C8-5 gel is elastic up to 70% strain and bounces back to its original shape when the load is removed (Fig. 7e). Furthermore, the C8-10 and C8-15 gels break at 26% and 20% strain, respectively. It can be concluded that the gels based on the quaternized C8 monomer are mechanically tougher relative to the gels based on the C4 and C6 monomers. This can be attributed to the presence of relatively more

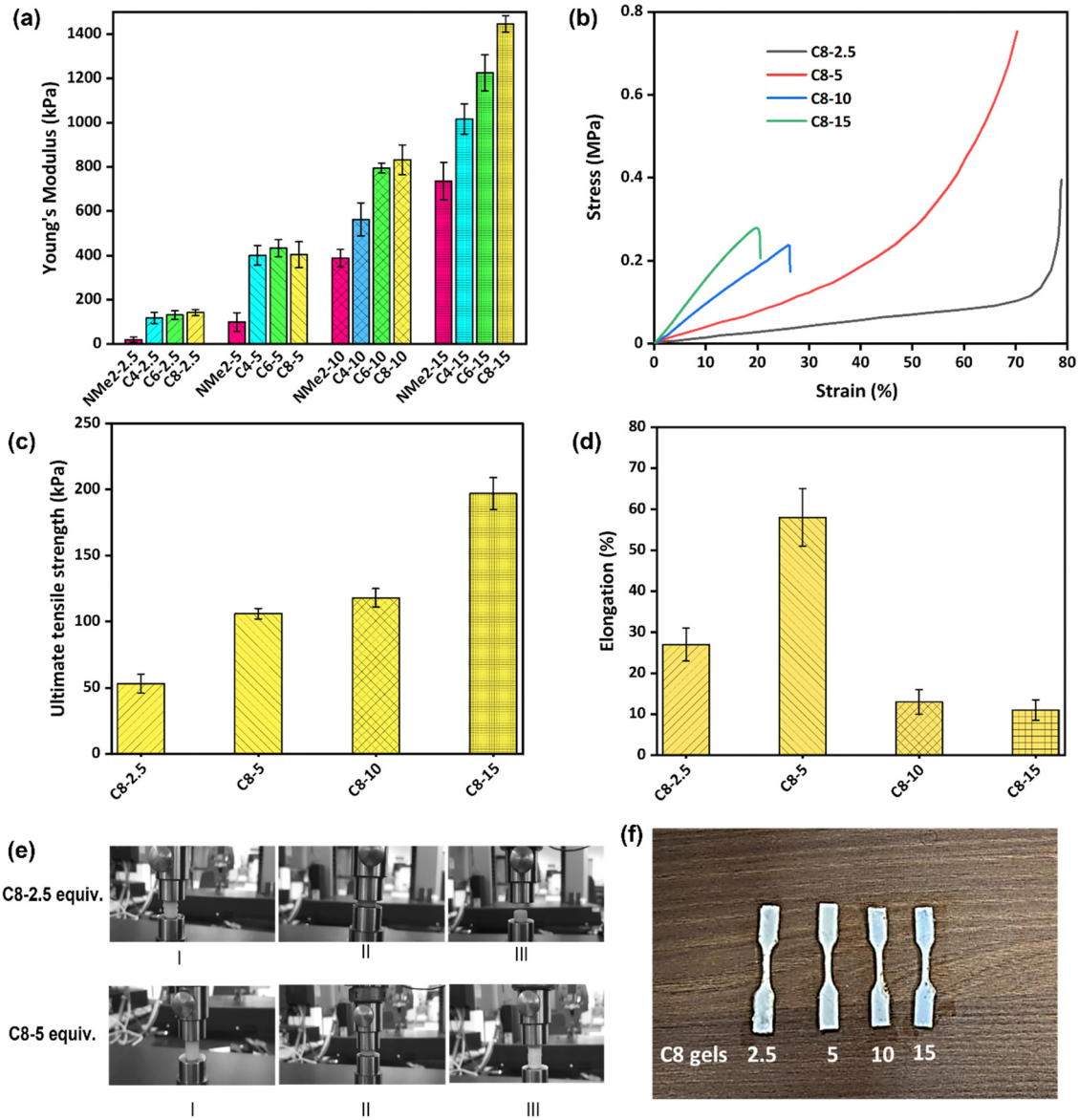

Fig. 7 (a) Young's modulus (*E*) for the MAPG bearing alkyl groups of different chain lengths and at varying crosslinking ratios subjected to compression tests. (b) Strain–Stress curve for the C8-2.5, C8-5, C8-10, and C8-15 gels subject to compression tests. (c) Ultimate tensile strength of the C8 gels. (d) % Elongation for the C8 gels. (e) Digital photograph of the C8-2.5 and C8-5 gels under compression, I-Initial state, II-under compression, III-after removal of load. (f) Digital photograph of the tensile sample for the C8-2.5, C8-5, C8-10, and C8-15 gels.

secondary hydrophobic interactions in the gels fabricated using the quaternized C8 monomers as compared to the C6 and C8 gels which are more brittle in nature and break at lower strain.[39–41]

Further, tensile testing has been done for the gel samples designated as C8-2.5, C8-5, C8-10, and C8-15, and the results are presented in Fig. 7(c and d), Fig. S15 and Table S3 (ESI†). In the case of the gel sample designated as C8-2.5, a tensile strength of 53 kPa was observed, which increases to 197 kPa on increasing the crosslinker amount to 15 eq. Furthermore, the elongation values for the gel samples designated as C8-2.5, C8-5, C8-10, and C8-15 are 27, 58, 12, and 11%, respectively. It can be seen that C8-5 is more stretchable as compared to the gels C8-2.5, C8-10, and C8-15, which is attributed to the octyl side chain as well as the optimized crosslinker amount of 5 eq.[42]

3.5. Antimicrobial study

The gels labeled as NMe2-2.5, NMe2-5, NMe2-10, NMe2-15, C4-2.5, C4-5, C4-10, C4-15, C6-2.5, C6-5, C6-10, C6-15, C8-2.5, C8-5, C8-10, C8-15 that differ in the alkyl chain length as well as the amount of crosslinker were evaluated for their antimicrobial activity against both Gram-positive and Gram-negative bacteria and the results are presented in Fig. 8 and are tabulated in Table 1. *Escherichia coli* and *Pseudomonas aeruginosa* were selected under Gram-negative bacteria, while *B. subtilis* and *S. aureus* were selected under Gram-positive bacteria. It is to be noted that the bacteria differ in their cell wall as well as cell

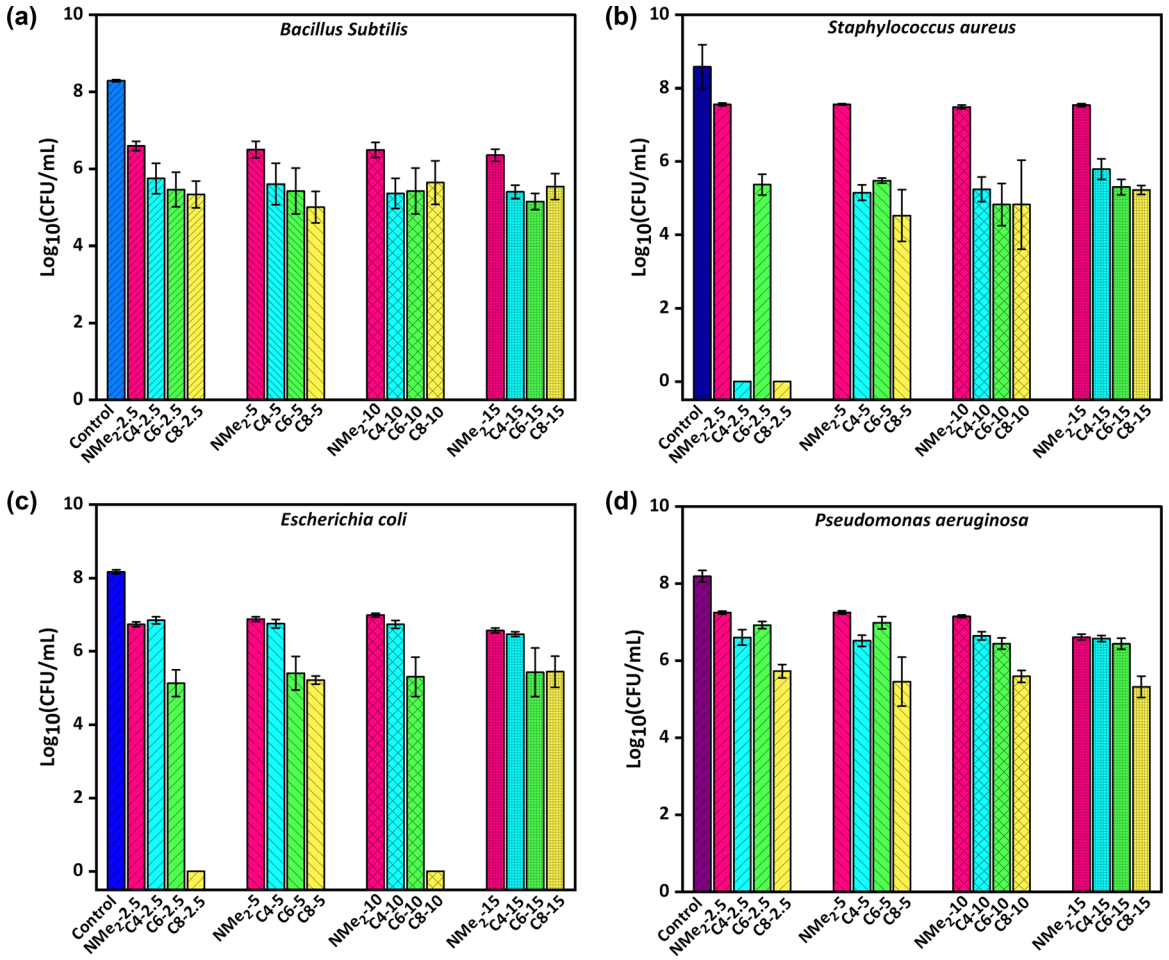

Fig. 8 Antimicrobial performance of the gels against (a) *B. subtilis* (b) *S. aureus* (c) *E. coli* and (d) *P. aeruginosa*. All data are presented as mean ± standard deviation (as indicated by error bars) based on values obtained from at least 3 biological replicates.

morphology, where *Staphylococcus aureus* exhibits a cocci shape while the remaining three have rod shapes. Depending upon the cellular morphology, the contact of the bacterium with the gel can differ resulting in differences in viability. It is expected that the gel network with a longer alkyl chain on the quaternary ammonium group will show high antimicrobial performance which is attributed to its enhanced interaction with the hydrophobic bacterial cell wall. In addition, the morphology of the gels and the quaternary ammonium monomer fraction contributes to the antimicrobial performance of the gels. It was observed that the NMe2 gels were able to display 85–94% reduction in the CFU (colony forming units) for *E. coli*, 73–93% for *P. aeruginosa*, 52–59% for *S. aureus*, and 94–97% for *B. subtilis*. Further, increasing the crosslinker amount in the NMe2 gels from 2.5 eq. to 10 eq., resulted in the reduction of the antimicrobial activity from 91 to 85% for *E. coli* and was attributed to a decrease in the fraction of amine moieties. Interestingly, antimicrobial activity was found to increase with an increase in the crosslinker to 15 eq. which has been ascribed to a decrease in pore size that leads to bacteria trapping inside the gels which ultimately results in the inactivation of the bacteria due to hydrophobic interactions. A similar trend was observed in the treatment of *P. aeruginosa* and *B. subtilis* with the gels labeled as NMe2. However, no clear trend was observed after the treatment of *S. aureus* bacteria with the NMe2 gels, which has been attributed to the morphology of bacteria.

The quaternized gels labeled as C4, C6, and C8 were also evaluated for their antimicrobial performance, where a reduction in the CFU (colony forming units) was higher and was related to the unquaternized NMe2 gels. On increasing the chain length of alkyl substitution from C4 to C8, the antimicrobial performance was found to be enhanced. These quaternized gels inactivate bacteria by electrostatic interactions of the ammonium cation with anions on the bacteria cells followed by interaction of the alkyl chain with the hydrophobic cell wall.

In the case of *E. coli*, an 89–95% reduction was observed with the butyl group, >99% reduction was observed with the hexyl group, and 99–100% reduction was observed with the octyl group containing quaternized polymeric gels. Further, the crosslinker amount was found to significantly influence the antimicrobial activity against *E. coli* for the quaternized gels functionalized with the butyl substituent, and on increasing the crosslinker ratio from 2.5 to 15 eq. the percentage reduction in the colony of *E. coli* was found to vary from 89 to 95%. This can be explained in terms of a

drastic reduction in the pore size of the C4 gels on increasing the crosslinker amount which leads to higher interaction between bacteria and gels.

The antimicrobial performance against *P. aeruginosa* was found to be similar for the C4 and C6 gels, where a maximum of 95% reduction was observed. It has been previously reported that the behaviour of *P. aeruginosa* is not dependent on alkyl chain length.[43] In addition, it has been suggested that *P. aeruginosa* shows less susceptibility to antibiotics due to poor membrane permeability. However, the quaternized gels containing the octyl group resulted in a more than 99% reduction of *P. aeruginosa*, which could be attributed to the small pore size as well as the optimum chain length of octyl to inactivate *P. aeruginosa.* Moreover, changing the crosslinker amount displayed a slight effect on the antimicrobial activity of the quaternized gels functionalized with hexyl chains against *P. aeruginosa*. It was revealed that, on increasing the crosslinker amount from 2.5 to 15 eq., the percentage reduction in the CFU (colony forming units) of *P. aeruginosa* vary from 79.27 to 95.77% for the quaternized C6 gels.

The antimicrobial performance of all quaternized polymeric gels against *B. subtilis* displayed a percentage reduction of

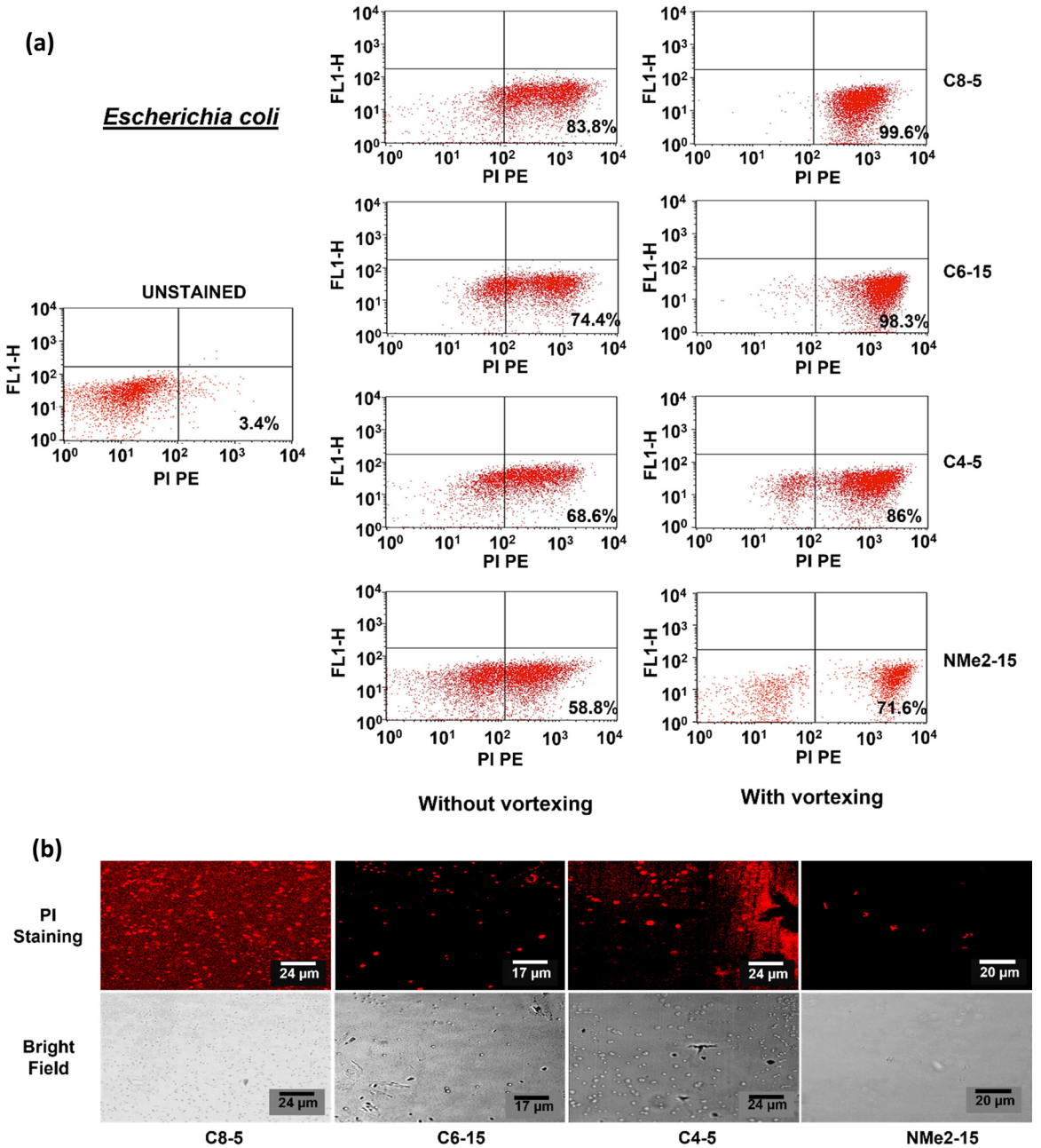

Fig. 9 (a) Flow cytometry was performed using PI stain with *E. coli* treated with different polymeric gels. (b) Confocal microscopy was performed using PI stain with *E. coli* treated with different polymeric gels.

>99% which remained the same on varying the degrees of crosslinking and alkyl chain length. In addition, the antimicrobial performance against all quaternized polymeric gels displayed a 99–100% reduction in bacteria. It is to be noted that, no clear trends of the effect of crosslinker amount on antimicrobial activity were observed with both *B. subtilis* and *S. aureus*.

From these results, it can be concluded that the gels containing alkyl chain groups ranging from C4 to C8 are particularly effective for Gram-positive bacteria. Further, the quaternized polymeric gels designated as C8-2.5, C8-5, C8-10, and C8-15 appear to be more promising as they resulted in a more than 99.5% reduction with all four bacterial strains *E. coli, P. aeruginosa, S. aureus*, and *B. subtilis*. It is clear from this that the key factor affecting the antibacterial action of the gel is the length of the alkyl chain. This outcome was in line with the findings of the earlier investigation, which showed

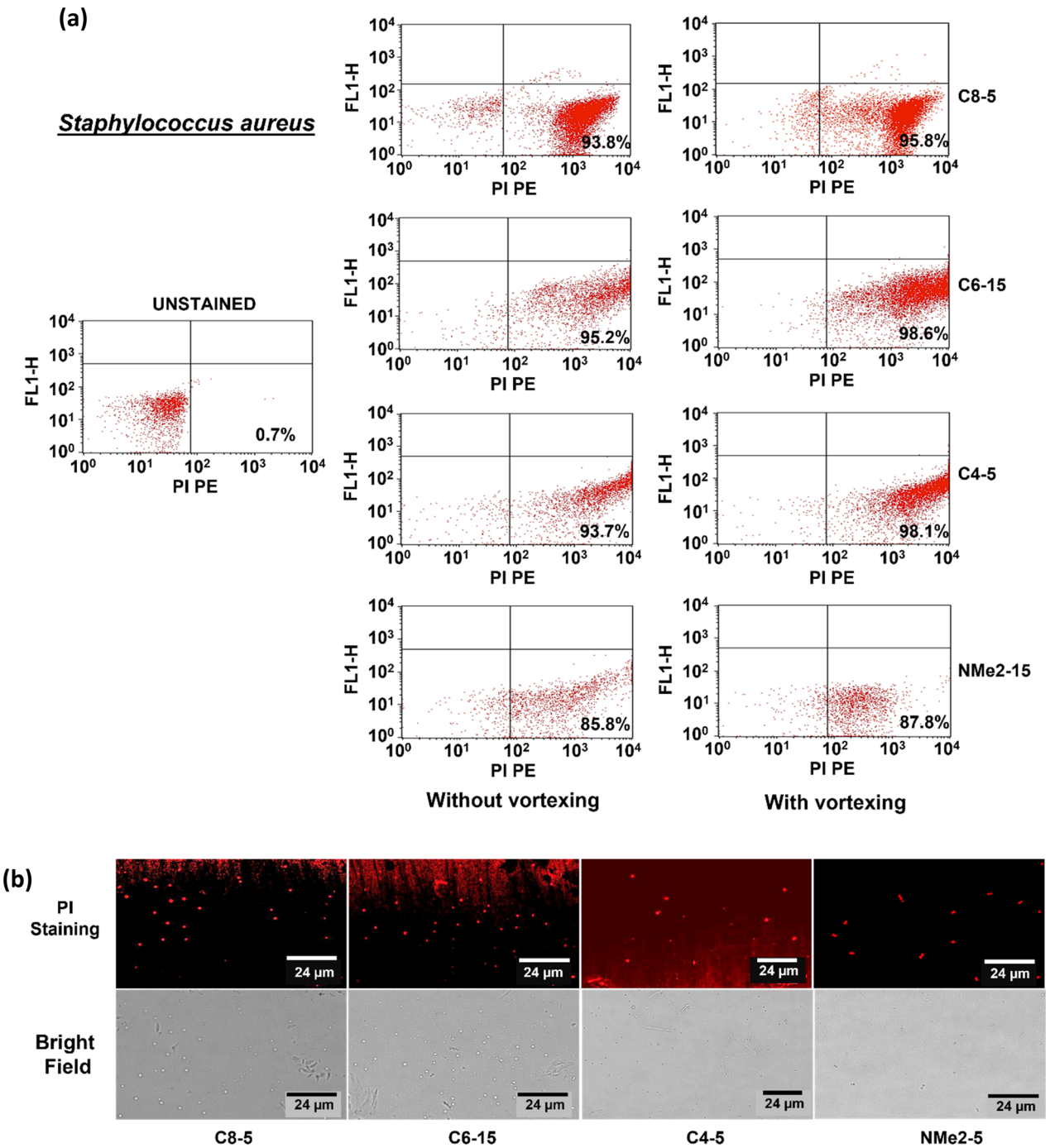

Fig. 10 (a) Flow cytometry was performed using PI stain with *S. aureus* treated with different polymeric gels. (b) Confocal microscopy was performed using PI stain with *S. aureus* treated with different polymeric gels.

that the quaternary ammonium derivative with a longer chain length was superior to the one with a shorter chain which is attributed to its enhanced interaction with hydrophobic bacterial cell wall, which causes the rupture of the membrane. However, in some cases, the crosslinker amount also has an effect on the antimicrobial activity of the gels, which could be attributed to the morphology of the gels and the fraction of active functionality in the gels.

3.6. Flow cytometry

To determine the mechanism of antimicrobial activity of the polymeric gels, flow cytometry was performed on two representative bacterial strains differing with respect to cell membrane, one Gram-positive and one Gram-negative namely *Escherichia coli* and *Staphylococcus aureus* respectively. A membrane-permeating propidium iodide (PI) dye was used which binds to DNA and gives red fluorescence. The dye is impermeable to the cell membrane and can pass through only compromised membranes. In the flow cytometry data, the lower left (LL) quadrant represents the unstained cells and the lower right (LR) quadrant represents the cells stained with PI dye. In the control, the untreated cells showed 0.7% and 3.5% dead cells in the case of *E. coli* and *S. aureus* respectively. After treatment with the gels, the fluorescence intensity in the FL1 channel increased showing cell lysis or cell death. In the *E. coli* cells treated with polymeric gels containing the octyl group as shown in Fig. 9, the signal increased in the LR to 83.8% and 99.6% without and with vortexing, respectively. The signals after the treatment of *E. coli* with the polymeric gels containing the hexyl group increased to 74.4% and 98.3% without and with vortexing respectively. Similarly, with the polymeric gels containing the butyl group, the cells which had taken up the PI stain were found to be 68.6 and 86.0% without and with vortexing respectively. On the other hand, with NMe2 gels, about 52.8% and 73.6% of the cells had taken up the stain without and with vortexing respectively. The results clearly demonstrate that the dead bacterial cells were trapped in the polymeric gels containing the alkyl group and were released after vortexing resulting in an increase in the stained cell population after vortexing. To visualize the trapped cells on the gel, confocal microscopy was performed. The PI-stained cells showed red fluorescence. Also, the cells appeared to be deformed, coccoid, or short rod shaped. A lot of the background appeared stained. It is likely that the DNA released from the lysed cells had taken up the stain.

In the case of *S. aureus* treated with polymeric gels containing the octyl group as shown in Fig. 10, the signal increased to 93.8% and 95.8% without and with vortexing, respectively. The signals after treatment with polymeric gels containing the hexyl group increased to 95.2% to 98.6% without and with vortexing. The signals after treatment with the polymeric gels containing the butyl group increased to 93.72% to 98.10% without and with vortexing, respectively. With the NMe2 gels, the population of cells that had taken up the stain was 85.8% and 87.8% without and with vortexing, respectively. It is noteworthy to mention that *S. aureus* cells did not show much difference with or without vortexing. The results also validate that the polymeric gels containing the alkyl groups were more effective than the NMe_2 gels. To visualize the cells confocal microscopy was performed. The cells appeared round but had taken up the PI stain, suggesting that the membrane structure was affected.

4. Conclusions

Macroporous antimicrobial polymeric gels were synthesized using a quaternary ammonium monomer varying in aliphatic chain length as well as the amount of crosslinker (OEG-DMA). Morphological analysis using FESEM confirms the macroporous structure of the gels. The antimicrobial activity of the polymeric gels was found to be highest for the gels synthesized using a quaternary ammonium monomer containing a C8 alkyl chain length. In addition to this, the mechanical performance also improved drastically on going from the gels synthesized using a quaternary ammonium monomer containing a C4 alkyl chain length to the gels synthesized using a quaternary ammonium monomer containing a C8 alkyl chain length which exhibits a Young's modulus of 1446 ± 38 kPa. This can be attributed to the improved compressive load dissipation on increasing the flexible alkyl chain length. The water uptake analysis in terms of the swelling degree has been quantified and was found to be the highest for the gels synthesized using a quaternary ammonium monomer containing a C4 alkyl chain length system in view of the relatively lower hydrophobicity of the material. The effect of the crosslinker ratio on the antimicrobial activity and the mechanical properties have also been examined. It was found that increasing the crosslinker ratio results in an increase in the Young's modulus. Furthermore, the effect of the crosslinker ratio on the antimicrobial properties was observed only with gels containing the butyl group, and the antimicrobial activity increased with increasing the crosslinker ratio from 2.5 eq. to 15 eq. However, for gels with the hexyl and octyl groups, the gels remain effective at all crosslinker ratios.

Conflicts of interest

There are no conflicts to declare.

Acknowledgements

LN and PS acknowledge the Science and Engineering Research Board, Department of Science and Technology for financial support in the form of a core research grant (CRG/2020/002055).

References

1 S. Levin, The crisis in antibiotic resistance, *Infect. Dis. Clin. Pract.*, 1993, **2**, 53.
2 S. B. Levy and M. Bonnie, Antibacterial resistance worldwide: Causes, challenges and responses, *Nat. Med.*, 2004, **10**, S122–S129.

3 C. Willyard, Drug-resistant bacteria ranked, *Nature*, 2017, **543**, 15.
4 K. Kümmerer, Resistance in the environment, *J. Antimicrob. Chemother.*, 2004, **54**, 311–320.
5 G. D. Wright, Antibiotic Adjuvants: Rescuing Antibiotics from Resistance, *Trends Microbiol.*, 2016, **24**, 862–871.
6 J. L. Armstrong, D. S. Shigeno, J. O. N. J. Calomiris and R. J. Seidler, Antibiotic-Resistant Bacteria in Drinking Water Antibiotic-Resistant Bacteria in Drinking Watert, *Appl. Environ. Microbiol.*, 2016, **42**, 277–283.
7 D. J. Payne, M. N. Gwynn, D. J. Holmes and D. L. Pompliano, Drugs for bad bugs: Confronting the challenges of antibacterial discovery, *Nat. Rev. Drug Discovery*, 2007, **6**, 29–40.
8 M. H. Kollef, Limitations of Vancomycin in the Management of Resistant Staphylococcal Infections, *Clin. Infect. Dis.*, 2007, **45**, S191–S195.
9 R. Namivandi-Zangeneh, R. J. Kwan, T. K. Nguyen, J. Yeow, F. L. Byrne, S. H. Oehlers, E. H. H. Wong and C. Boyer, The effects of polymer topology and chain length on the antimicrobial activity and hemocompatibility of amphiphilic ternary copolymers, *Polym. Chem.*, 2018, **9**, 1735–1744.
10 S. Krishnan, R. J. Ward, A. Hexemer, K. E. Sohn, K. L. Lee, E. R. Angert, D. A. Fischer, E. J. Kramer and C. K. Ober, Surfaces of fluorinated pyridinium block copolymers with enhanced antibacterial activity, *Langmuir*, 2006, **22**, 11255–11266.
11 Y. Oda, S. Kanaoka, T. Sato, S. Aoshima and K. Kuroda, Block versus random amphiphilic copolymers as antibacterial agents, *Biomacromolecules*, 2011, **12**, 3581–3591.
12 G. Sauvet, W. Fortuniak, K. Kazmierski and J. Chojnowski, Amphiphilic block and statistical siloxane copolymers with antimicrobial activity, *J. Polym. Sci., Part A: Polym. Chem.*, 2003, **41**, 2939–2948.
13 R. T. C. Cleophas, J. Sjollema, H. J. Busscher, J. A. W. Kruijtzer and R. M. J. Liskamp, Characterization and activity of an immobilized antimicrobial peptide containing bactericidal PEG-hydrogel, *Biomacromolecules*, 2014, **15**, 3390–3395.
14 S. J. Lam, N. M. O'Brien-Simpson, N. Pantarat, A. Sulistio, E. H. H. Wong, Y. Y. Chen, J. C. Lenzo, J. A. Holden, A. Blencowe, E. C. Reynolds and G. G. Qiao, Combating multidrug-resistant Gram-negative bacteria with structurally nanoengineered antimicrobial peptide polymers, *Nat. Microbiol.*, 2016, **1**, 16162.
15 L. Jiang, D. Xu, T. J. Sellati and H. Dong, Self-assembly of cationic multidomain peptide hydrogels: Supramolecular nanostructure and rheological properties dictate antimicrobial activity, *Nanoscale*, 2015, **7**, 19160–19169.
16 A. G. Gallagher, J. A. Alorabi, D. A. Wellings, R. Lace, M. J. Horsburgh and R. L. Williams, A Novel Peptide Hydrogel for an Antimicrobial Bandage Contact Lens, *Adv. Healthcare Mater.*, 2016, **5**, 2013–2018.
17 X. Li, S. M. Robinson, A. Gupta, K. Saha, Z. Jiang, D. F. Moyano, A. Sahar, M. A. Riley and V. M. Rotello, Functional gold nanoparticles as potent antimicrobial agents against multidrug-resistant bacteria, *ACS Nano*, 2014, **8**, 10682–10686.
18 S. L. Loo, A. G. Fane, T. T. Lim, W. B. Krantz, Y. N. Liang, X. Liu and X. Hu, Superabsorbent cryogels decorated with silver nanoparticles as a novel water technology for point-of-use disinfection, *Environ. Sci. Technol.*, 2013, **47**, 9363–9371.
19 M. E. Davis, Z. Chen and D. M. Shin, Nanoparticle therapeutics: An emerging treatment modality for cancer, *Nat. Rev. Drug Discovery*, 2008, **7**, 771–782.
20 M. Auffan, J. Rose, J. Y. Bottero, G. V. Lowry, J. P. Jolivet and M. R. Wiesner, Towards a definition of inorganic nanoparticles from an environmental, health and safety perspective, *Nat. Nanotechnol.*, 2009, **4**, 634–641.
21 S. J. Shirbin, S. J. Lam, N. J. A. Chan, M. M. Ozmen, Q. Fu, N. O'Brien-Simpson, E. C. Reynolds and G. G. Qiao, Polypeptide-Based Macroporous Cryogels with Inherent Antimicrobial Properties: The Importance of a Macroporous Structure, *ACS Macro Lett.*, 2016, **5**, 552–557.
22 D. S. S. M. Uppu, M. Bhowmik, S. Samaddar and J. Haldar, Cyclization and unsaturation rather than isomerisation of side chains govern the selective antibacterial activity of cationic-amphiphilic polymers, *Chem. Commun.*, 2016, **52**, 4644–4647.
23 Y. Wang, S. Gao, W. H. Ye, H. S. Yoon and Y. Y. Yang, Co-delivery of drugs and DNA from cationic core–shell nanoparticles self-assembled from a biodegradable copolymer, *Nat. Mater.*, 2006, **5**, 791–796.
24 D. S. S. M. Uppu and J. Haldar, Lipopolysaccharide Neutralization by Cationic-Amphiphilic Polymers through Pseudoaggregate Formation, *Biomacromolecules*, 2016, **17**, 862–873.
25 B. Findlay, G. G. Zhanel and F. Schweizer, Cationic amphiphiles, a new generation of antimicrobials inspired by the natural antimicrobial peptide scaffold, *Antimicrob. Agents Chemother.*, 2010, **54**, 4049–4058.
26 H. Takahashi, E. T. Nadres and K. Kuroda, Cationic Amphiphilic Polymers with Antimicrobial Activity for Oral Care Applications: Eradication of S. mutans Biofilm, *Biomacromolecules*, 2017, **18**, 257–265.
27 D. S. S. M. Uppu, M. M. Konai, U. Baul, P. Singh, T. K. Siersma, S. Samaddar, S. Vemparala, L. W. Hamoen, C. Narayana and J. Haldar, Isosteric substitution in cationic-amphiphilic polymers reveals an important role for hydrogen bonding in bacterial membrane interactions, *Chem. Sci.*, 2016, **7**, 4613–4623.
28 I. Mukherjee, A. Ghosh, P. Bhadury and P. De, Side-Chain Amino Acid-Based Cationic Antibacterial Polymers: Investigating the Morphological Switching of a Polymer-Treated Bacterial Cell, *ACS Omega*, 2017, **2**, 1633–1644.
29 K. Zhang, L. Cheng, M. D. Weir, Y. X. Bai and H. H. K. Xu, Effects of quaternary ammonium chain length on the antibacterial and remineralizing effects of a calcium phosphate nanocomposite, *Int. J. Oral Sci.*, 2016, **8**, 45–53.
30 T. Zhao and G. Sun, Hydrophobicity and antimicrobial activities of quaternary pyridinium salts, *J. Appl. Microbiol.*, 2008, **104**, 824–830.
31 P. Sahariah, B. E. Benediktssdóttir, M. A. Hjálmarsdóttir, O. E. Sigurjonsson, K. K. Sørensen, M. B. Thygesen, K. J. Jensen and M. Másson, Impact of chain length on antibacterial activity and hemocompatibility of quaternary

N-alkyl and *N*,*N*-dialkyl chitosan derivatives, *Biomacromolecules*, 2015, **16**, 1449–1460.

32 A. Kumar, C. Boyer, L. Nebhani and E. H. H. Wong, Highly Bactericidal Macroporous Antimicrobial Polymeric Gel for Point-of-Use Water Disinfection, *Sci. Rep.*, 2018, **8**, 1–9.

33 S. L. Loo, W. B. Krantz, T. T. Lim, A. G. Fane and X. Hu, Design and synthesis of ice-templated PSA cryogels for water purification: Towards tailored morphology and properties, *Soft Matter*, 2013, **9**, 224–234.

34 V. I. Lozinsky, Cryogels on the basis of natural and synthetic polymers: Preparation, properties and application, *Usp. Khim.*, 2002, **71**, 579–584.

35 V. I. Lozinsky, Polymeric cryogels as a new family of macroporous and supermacroporous materials for biotechnological purposes, *Russ. Chem. Bull.*, 2008, **57**, 1015–1032.

36 J. Wolfe, G. Bryant and K. L. Koster, What is 'unfreezable water', how unfreezable is it and how much is there?, *CryoLetters*, 2002, **23**, 157–166.

37 S. L. Loo, W. B. Krantz, T. T. Lim, A. G. Fane and X. Hu, Design and synthesis of ice-templated PSA cryogels for water purification: Towards tailored morphology and properties, *Soft Matter*, 2013, **9**, 224–234.

38 Y. Liu, Z. Li, J. Xu, B. Wang, F. Liu, R. Na, S. Guan and F. Liu, Effects of amphiphilic monomers and their hydrophilic spacers on polyacrylamide hydrogels, *RSC Adv.*, 2019, **9**, 3462–3468.

39 Y. Gao, L. Duan, S. Guan, G. Gao, Y. Cheng, X. Ren and Y. Wang, The effect of hydrophobic alkyl chain length on the mechanical properties of latex particle hydrogels, *RSC Adv.*, 2017, **7**, 44673–44679.

40 J. Pan, L. Gao, W. Sun, S. Wang and X. Shi, Length Effects of Short Alkyl Side Chains on Phase-Separated Structure and Dynamics of Hydrophobic Association Hydrogels, *Macromolecules*, 2021, **54**, 5962–5973.

41 C. K. Chen, P. W. Chen, H. J. Wang and M. Y. Yeh, Alkyl chain length effects of imidazolium ionic liquids on electrical and mechanical performances of polyacrylamide/alginate-based hydrogels, *Gels*, 2021, **7**, 164.

42 X. Yan, Q. Chen, L. Zhu, H. Chen, D. Wei, F. Chen, Z. Tang, J. Yang and J. Zheng, High strength and self-healable gelatin/polyacrylamide double network hydrogels, *J. Mater. Chem. B*, 2017, **5**, 7683–7691.

43 P. Sahariah, B. E. Benediktssdóttir, M. A. Hjálmarsdóttir, O. E. Sigurjonsson, K. K. Sørensen, M. B. Thygesen, K. J. Jensen and M. Másson, Impact of chain length on antibacterial activity and hemocompatibility of quaternary *N*-alkyl and *N*,*N*-dialkyl chitosan derivatives, *Biomacromolecules*, 2015, **16**, 1449–1460.

